Effects of Ultraviolet Radiation Exposure on Vinyl Ester Matrix Resins: Chemical and Mechanical Characterization

A. W. Signor and J. W. Chin

ABSTRACT

The increased use of fiber-reinforced vinyl ester composites in outdoor applications has led to questions concerning the environmental durability of these materials, particularly as related to UV exposure. In this work, artificial ultra-violet (UV) degradation was carried out on neat vinyl ester matrix specimens using an integrating sphere-based UV exposure chamber. Significant changes were observed in the bulk mechanical properties, surface chemistry, and surface topography after 1000 h and 4000 h of exposure. ASTM D 638 Type-V specimens with a nominal thickness of 1.6 mm were tested in tension. A transition from slightly ductile to brittle behavior was observed along with a decrease of up to 40% in average strain-to-failure and a decrease of up to 60% in the average specific toughness (toughness normalized to cross-sectional area) after exposure. Changes in the hardness and modulus of the surface after exposure were studied by using an atomic force microscope (AFM) nanoindentation technique. A significant increase in the apparent hardness of the exposed surface was accompanied by an increase in the apparent Young's modulus of the near-surface region. Topographical changes, including an increase in both the number and size of surface defects on the exposed surface were observed using optical microscopy and tapping-mode AFM. Chemical changes in the exposed surfaces were also observed using Fourier-Transform Infrared – Attenuated Total Reflectance (FTIR-ATR) spectroscopy.

Building Materials Division, National Institute of Standards and Technology, Gaithersburg, MD 20899

INTRODUCTION

The use of polymer matrix composites in building and construction has become attractive due to the many advantages offered by composite materials. Among these advantages are excellent corrosion resistance and a high strength-to-weight ratio. However, the outdoor environment contains several elements that are destructive to organic polymers, such as moisture, acid rain, temperature cycling, and ultraviolet (UV) radiation. Out of all of the environmental stresses, UV radiation is potentially the most damaging to polymeric materials.

The primary objective of this study was to investigate the chemical and mechanical effects of UV radiation on vinyl ester, a matrix polymer commonly used in infrastructure composites. Effects of exposure to UV radiation from a 1000 W xenon arc source were characterized by tensile testing, atomic force microscopy (AFM), and Fourier-transform infrared spectroscopy (FTIR). Nanoindentation was performed with the AFM on exposed and unexposed surfaces to measure changes in the hardness and Young's modulus in the exposed surface. The AFM was also used to monitor changes in the surface topography on the nanometer level. This combination of mechanical, chemical, and microscopic analysis was used to obtain an understanding of the degree to which this resin system degrades under exposure to UV radiation, and to determine UV degradation effects on bulk tensile properties.

EXPERIMENTAL

Specimen Preparation

All specimens were fabricated from Derakane 411-350 PA[*] vinyl ester resin, cured with 3 mass % methyl ethyl ketone peroxide (MEKP) catalyst and containing 0.02 mass % SAG 47 silicone antifoaming agent. Once formulated, the resin was allowed to cure for 24 h at room temperature followed by a 2 h po st-cure at 150 ^{o}C. Specimens were prepared in two different forms: ASTM D 638 Type-V specimens (nominally 1.6 mm thick) and 60 mm x 60 mm x 1.6 mm cast sheets for AFM and FTIR-ATR analysis. Both specimen forms were manufactured via a modified injection-molding process. In both cases, the mold consisted of a silicone rubber gasket sandwiched between two poly(methyl methacrylate) platens lined with Mylar release film. In the case of the cast sheet, one large (60 mm x 60 mm) opening was cut from the gasket. In the case of the tensile specimens, cavities were punched out of the gasket using an ASTM D 638 Type-V punch. The tensile specimens were produced in groups of six, each group being from the same batch of catalyzed resin. Several 10 mm x 10 mm specimens for AFM/FTIR-ATR analysis were cut from the 60 mm x 60 mm cast sheet by scoring with a razor blade.

---

[*] Note: Certain commercial equipment, instruments or materials are identified in this paper in order to specify the experimental procedure adequately. Such identification is not intended to imply recommendation or endorsement by the National Institute of Standards and Technology, nor is it intended to imply that the materials or equipment identified are necessarily the best available for this purpose.

Ultraviolet Radiation Exposure

Exposures were carried out using a 1000 W xenon arc lamp from Oriel coupled with a 0.3 m diameter integrating sphere, as shown in Figure 1. An integrating sphere is a hollow spherical chamber that has a highly diffuse reflecting inner surface. The optimal inner surface coating, for UV applications, is fabricated from pressed polytetrafluoroethylene powder or bulk fluoropolymers, both having greater than 98% reflectance at UV wavelengths longer than 280 nm [1]. When radiation enters an integrating sphere, the radiation is diffusely reflected from the interior surface. After multiple reflections, the radiation inside the sphere becomes spatially integrated, highly uniform, and has an increased irradiance that is directly proportional to the total radiation flux entering the sphere. With proper design, the radiation exiting a port machined through the wall of an integrating sphere is extremely uniform over the dimensions of the port [1].

In addition to irradiance non-uniformity, a lack of sample temperature control can also lead to a lack of both repeatability and reproducibility, therefore methods were taken to control sample temperature [1]. The lamp system used in this study contained a dichroic mirror positioned between the xenon light source and the integrating sphere, which reflected the UV component of the radiation emitted from the lamp into the sphere and transmitted the visible and infrared portions to a heat sink. The use of the dichroic mirror removes the infrared radiation, the primary source of thermal energy in an optical system, and thus limits sample heating. During exposure, the samples were mounted in two 10 cm diameter ports on opposite sides of the integrating sphere. The light source was characterized using a Hewlett Packard 8452A spectrophotometer with a diffusing probe; spectra were taken systematically at 33 points across the open area of each port. This was done to characterize the spectral irradiance of the ports and to determine if any irradiance non-uniformity existed either within the individual ports or between the two different ports. Some representative spectra are shown in Figure 2.
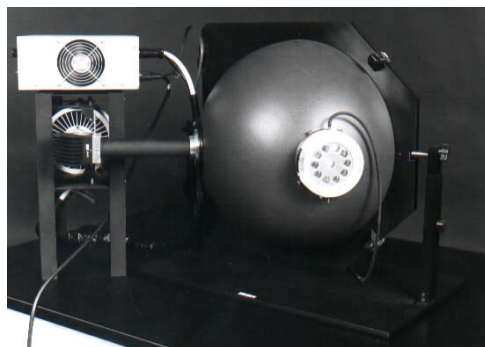
Figure 1: An integrating-sphere-based UV exposure chamber.
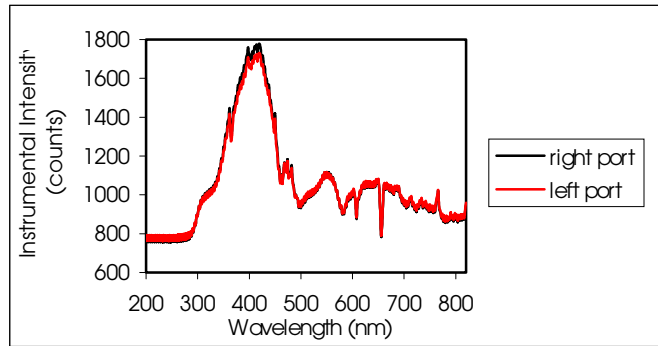
Figure 2: Comparison of spectral output from the right and left port of the integrating sphere.

For both the left and right ports, all 33 spectra were superimposable. Figure 2 shows the spectra collected at a common point at each port. No significant irregularity was found within the ports, and only minor discrepancies were measured between the two different ports.

The exposure was carried out in an ambient atmosphere where the temperature was nominally 22 ^{o}C – 24 ^{o}C, with a humidity of 30 %-50 %. A set of control samples (twelve tensile specimens, one AFM specimen, one FTIR-ATR specimen) were not exposed to UV and were stored in a dark drawer prior to analysis. One set of samples (ten tensile specimens, one AFM specimen, and one FTIR-ATR specimen) was removed from the integrating sphere after 1002 h (hereafter referred to as 1000 h) and then stored with the control specimens. The third set of specimens (ten tensile specimens, one AFM specimen, and one FTIR-ATR specimen) was removed after 3939 h (hereafter referred to as 4000 h) of exposure and stored with the control specimens until analysis. The samples were randomized with respect to both exposure time and integrating sphere location, in order to minimize any formulation or irradiance non-uniformity effects on data trends.

Tensile Testing

Tensile testing of ASTM D 638 Type-V samples was carried out on a screw-driven Instron 1125 universal testing machine with manually tightened grips at a constant crosshead speed of 1 mm/min. A torque wrench was used to tighten the grips consistently between samples. Due to the fact that no appropriate extensometer was available, the grip separation was used as the gauge length for measuring extension. A computer software package was used for instrument control, data acquisition, and calculation of all material tensile properties. Engineering stress (σ_e) engineering strain (ε_e), peak load, Young's modulus (although only an estimate due to the lack of extensometer), and specific toughness (energy to break per unit cross-sectional area) were measured. Nine replicates were tested for both the 1000 h and 4000 h specimen sets, while twelve replicates of the control specimens were tested.

Nanoindentation

Nanoindentation of exposed and unexposed surfaces was performed using a Digital Instruments Dimension 3100 AFM equipped with a diamond-tip, stainless steel cantilever probe with a spring-constant of 120 N/m ± 10 N/m (reported by manufacturer). This technique is described in more detail elsewhere [2]. The AFM software allowed control over the maximum indentation force. A compensating lateral motion was also used to reduce uncertainties due to lateral tip motion during the indentation process [2]. Indents were performed using four different maximum forces; data analysis is presented here only for the smallest force used, which was approximately 3630 nN. An array of multiple indents were created at different locations until a significant sampling of the entire 1 cm^2 specimen area was obtained. An unexposed control specimen was always analyzed alongside the 1000 h and 4000 h specimens.

Surface Topography

Microscopy of exposed and unexposed surfaces was carried out using both optical and AFM tapping-mode techniques. Optical micrographs of both exposed and unexposed surfaces were obtained using the optical system of the AFM. Tapping mode AFM was used to collect height and phase data in scan sizes ranging from 1 μm x 1 μm to 100 μm x 100 μm. Both steel and silicon cantilevers were used in tapping-mode imaging. In tapping mode, the cantilever tip is oscillated at its fundamental frequency, which is about 60 kHz for the stainless-steel cantilever, and about 300 kHz for the silicon cantilever. The oscillating tip is raster-scanned across the surface while a laser beam, reflected off the cantilever tip onto a photodiode detector, is used to monitor the oscillation amplitude. As with the indentation measurements, topographical scans were performed in several locations in order to obtain a significant sampling of the topographical changes induced by UV exposure.

Fourier Transform Infrared Spectroscopy

FTIR analysis of exposed and unexposed vinyl ester epoxy resin surfaces was performed using a Nicolet Magna-IR 560 spectrometer with an ASI ATR probe. The probe consisted of a zinc selenide focusing element and a diamond internal reflectance element. The probe geometry provided three reflections on the sample surface at an angle of incidence, θ, of 45°. By assuming a refractive index of the sample, n_1, of 1.5, the depth of penetration of the beam into the sample surface, D_p, as a function of wavelength, λ, was estimated as follows [3]:

$$D_p = \frac{\lambda}{2 n_1 \pi \left(Sin^2\theta - n_{21}^2 \right)^{\frac{1}{2}}} \tag{1}$$

Where: n_2 = refractive index of internal reflectance element

$$n_{21} = \frac{n_2}{n_1}$$

The probe was brought into intimate contact with the sample surface using mechanical pressure. 32 scans were collected over the spectral range of 400 cm^{-1}-4000 cm^{-1}. Both the probe and bench were purged with dry air and background spectra were collected before each sample spectrum was taken.

RESULTS AND DISCUSSION

Tensile Testing

Stress-strain curves for specimens tested after 0 h, 1000 h, and 4000 h of exposure are presented in Figures 3(a), 3(b), and 3(c). The unexposed material exhibited slightly ductile behavior, displaying a yield point and a small degree of plastic deformation. Little, if any, statistically significant changes in the tensile properties were observed after 1000 h of exposure; the stress-strain curves still showed significant yielding and plastic deformation. However, after 4000 h of irradiation, there was a definite transition from ductile to brittle behavior, as can be seen in the shapes of the stress-strain curves for the different irradiation times. Additional tensile properties are tabulated in Table I. The decrease in specific toughness and strain at break following UV exposure is graphically represented in Figure 3(d). The average ultimate engineering strain decreased from 16.7% for the unexposed material to 14.9% after 1000 h of exposure and 8.9% after 4000 h. The average specific toughness (total energy to break/unit cross-sectional area) decreased from 1.4 kg-mm/mm^2 for the unexposed material to 1.2 kg-mm/mm^2 after 1000 h of exposure and 0.56 kg-mm/mm^2 after 4000 h. Thus, after 4000 h of exposure, the strain-at-break decreased to approximately 40% of the original value and the specific toughness decreased to approximately 60% of the original value.

All of the changes in tensile properties indicate a transition from slightly ductile to brittle behavior as a result of increasing UV dosage. Specific toughness and ultimate strain were observed to be the most sensitive to UV-induced degradation.   It is likely that significant embrittlement of, or the creation of additional defects in, a thin surface layer could significantly reduce the energy required for a crack to nucleate and propagate through the bulk material. Thus, the observed change in bulk properties could actually be a result of the change in the mechanical properties of a thin UV-degraded surface layer.
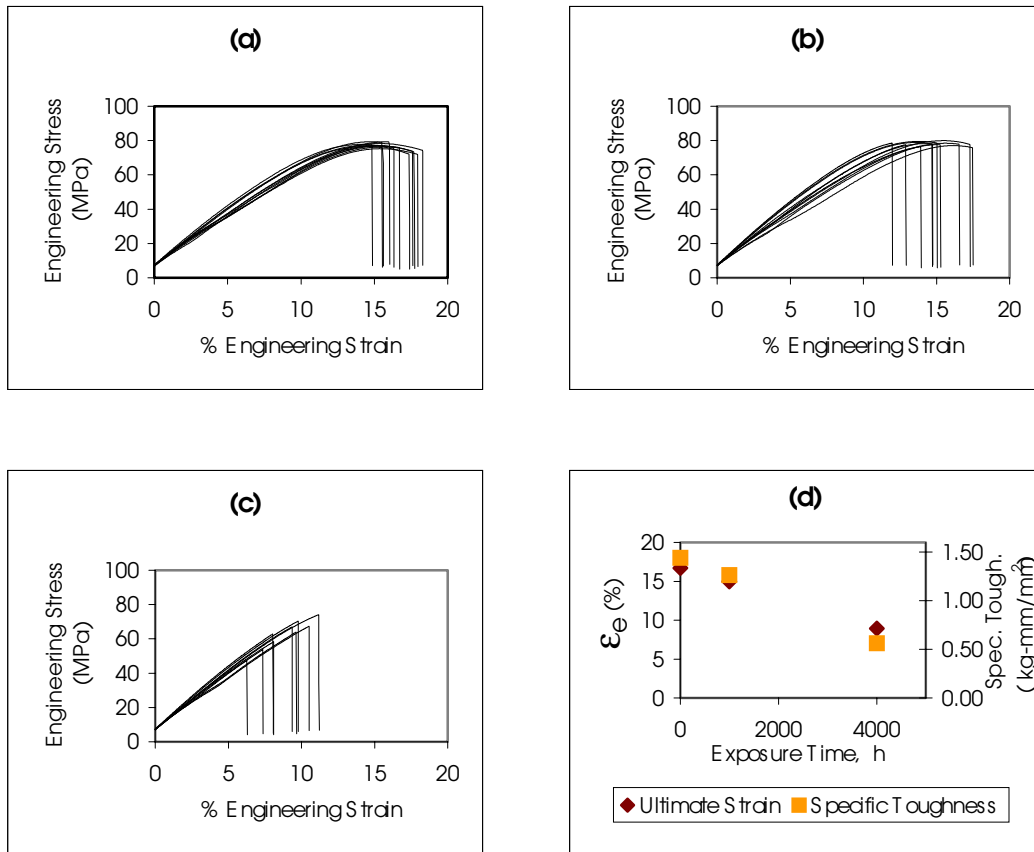
Figure 3: Stress-strain curves for (a) 0 h, (b) 1000 h, (c) 4000 h, and (d) Ultimate strain and specific toughness vs. exposure time.

TABLE I: Tensile properties of UV-exposed specimens

Exposure Time (h)	Ultimate ε_e (%)	E (MPa)	Peak σ_e (MPa)	Spec. Tough. (kg-mm/mm^2)
0	16.72 ± 1.14	654.67 ± 47.57	77.44 ± 1.22	1.44 ± 0.15
1000	14.98 ± 1.78	692.28 ± 71.39	78.24 ± 1.10	1.26 ± 0.19
4000	8.92 ± 1.59	696.67 ± 50.53	62.80 ± 8.38	0.56 ± 0.16

Nanoindentation

The first step in analyzing the nanoindentation data was to determine the approximately linear relationship between the tip deflection measured by the photodiode and the force applied to the sample. To measure the system sensitivity indentation was performed on a sapphire sample that was essentially infinitely stiff with respect to the cantilever probe, i.e. the tip did not penetrate the sapphire. Thus, the data acquired from such a process is assumed to be solely due to the bending of the cantilever and allows the photodiode signal to be calibrated in terms of distance

of tip displacement due to this bending. Knowing the spring constant of the cantilever, one can relate this tip displacement measured by the AFM to a force value. Further, this type of calibration allows the penetration of the tip into the sample to be calculated from the acquired tip deflection vs. scanner displacement data. A typical load vs. penetration curve for the vinyl ester specimen is shown in Figure 4.

Included in the analysis of the nanoindentation data were the determination of indent depth, which is related to hardness, and an estimate of the Young's modulus of the vinyl ester surface. The indent depth was taken as the maximum displacement value obtained in each indent. An accurate estimate of the Young's modulus was difficult to obtain due to the contributions of elastic, plastic, and viscoelastic deformation. Because the vinyl ester resin is a viscoelastic material, the portion of the load vs. displacement data most indicative of elasticity is the unloading curve near the maximum extension (i.e. just as the probe starts to retract out of the indent). This data represents the forces exerted by the cantilever during elastic recovery of the sample. A linear estimation of the slope, S, was conducted for the first ten data points of the unloading curve, which is schematically shown in Figure 4. As a general rule, the first ten data points were very nearly linear in force and displacement. The physical units of this linear best-fit slope are nN/nm; in order to estimate a modulus, one needs to consider the projected area of contact between the probe tip and the sample surface. The first step in calculating this area is to determine the relationship between the depth of penetration and the projected area. To calculate this relationship, *blind-reconstruction* data, or experimentally obtained tip geometry data, was used [4]. Once the projected area, A, was determined from the blind reconstruction data, an estimated modulus was calculated from elasticity theory.

The specific mathematical relationship used in estimating the Young's modulus, E, from the load-displacement and blind reconstruction data is shown as follows [4]:

$$S = 2\beta \left(\frac{E}{1-v^2} \right) \left(\frac{A}{\pi} \right)^{\frac{1}{2}} \tag{2}$$

Where: β = constant used to account for triangular and square indenter cross sections

v = Poisson's ratio of sample
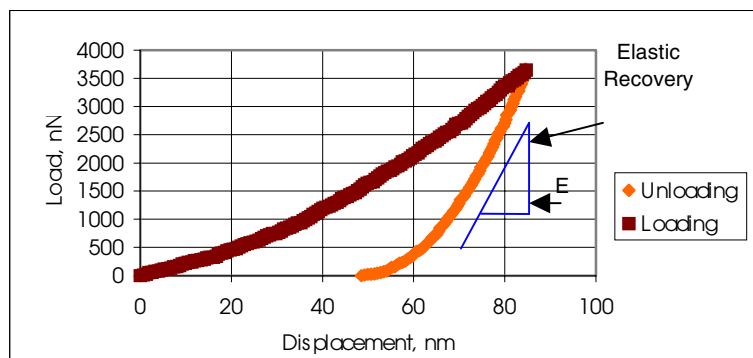
Figure 4: Typical load vs. displacement curve for vinyl ester resin.

The average indent depth and apparent Young's modulus for each set of specimens, as well as their standard deviations are shown in Table II. It must be understood that the Young's moduli reported here are not absolute values, but relative measures indicative of any change in the surface modulus upon UV exposure.

There was a significant decrease in indentation depth, as well as a significant increase in the estimated Young's modulus after 1000 h of exposure. After 4000 h of UV exposure, there was no indication of further change (taking into consideration the scatter in the data). The increased surface modulus due to UV irradiation is in agreement with both the increased nano-hardness and the brittle tensile behavior. It appears that after 1000 h of exposure (or earlier), no further change in the surface modulus or hardness occurs. This observation suggests that the degradation layer has grown deeper than the average indent depth of about 80 nm-90 nm. This is in agreement with studies that have reported that the degradation layer can grow to depths greater than 100 µm in short amounts of time [5]. An increased hardness and modulus at the exposed surface is indicative of embrittlement upon irradiation, which is consistent with the observed bulk tensile properties.

**TABLE II:** Nanoindentation Data for UV-exposed Vinyl Ester

| Exposure Time (h)	Indentation Depth (nm)	$E_{estimated}$ (MPa)
0	81.98 ± 8.60	1.23 ± 0.47
1000	51.97 ± 6.89	3.75 ± 1.32
4000	55.71 ± 5.16	2.32 ± 0.64

Topography

Several observations were made concerning topographical changes on the surface of the material upon irradiation. The first observation made was simply the macroscopic loss of luster. The exposed surfaces were less specularly reflective than the unexposed surfaces, and the interface between exposed and unexposed portions of both the 1000 h and 4000 h specimens (where a portion of each

specimen was shielded from the light by the mount) could be identified with the naked eye. Representative optical micrographs showing the evolution of defects on the surface of the resin with increasing UV dosage, are shown in Figure 5. The unexposed control surface is shown in Figure 5(a), and the surface after 1000 h of exposure is shown in Figure 5(c). Figure 5(b) shows the interface between the exposed and unexposed surfaces of the 1000 h specimen that could be discerned with the naked eye. As the pits and blisters increased in size and number, the scratch-like defects observed in the unexposed specimens appeared to "melt" away with increasing exposure time. After 4000 h, the size and number of pits continued to increase and large bull's eye-like and crosshatched defects on the size scale of 50 µm to100 µm were observed with the optical microscope, as is seen in Figure 5(d).

Tapping mode AFM with a silicon cantilever revealed the presence of tiny blister-like features on the order of 10 nm in diameter, with a few of these features reaching a height of 300 nm after 1000 h of exposure. The evolution of these defects on the surface is depicted in Figure 6. After 4000 h of exposure, the number and size of these protruding defects on the surface increased significantly, nearly all of them reaching a height of about 300 nm. After 4000 h of exposure, the density and size of these features fluctuated little across the entire exposed surface. These features could be due either to the accumulation of degradation products or to the ablation of the surface by the UV degradation.
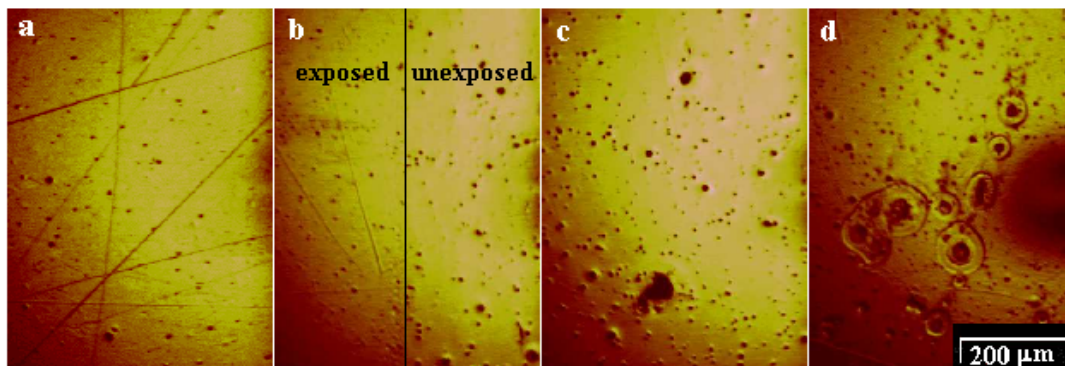
Figure 5: Optical micrographs of vinyl ester surface after (a) 0 h, (b) 1000 h at interface between unexposed and exposed surfaces, (c) 1000 h, and (d) 4000 h of exposure.
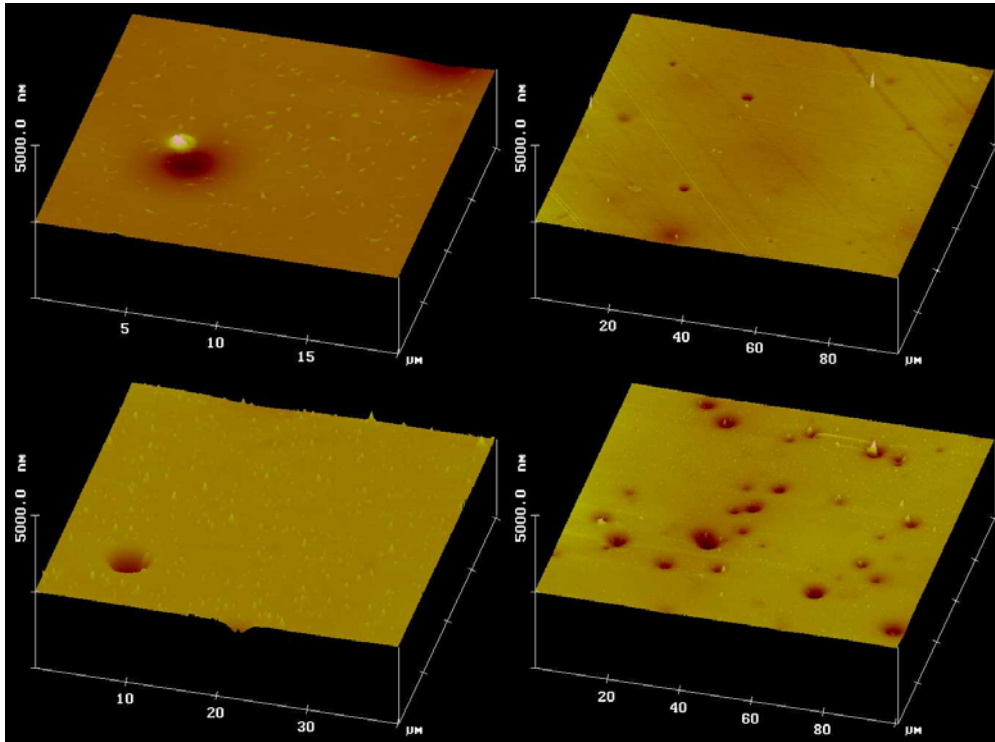
Figure 6: AFM tapping-mode images after (a) 0 h, (b) 1000 h, (c) 1000 h, and (d) 4000 h of exposure.

Fourier-Transform Infrared Spectroscopy

There were observable changes in the infrared absorption spectrum after 1000 h of exposure; however, no additional changes were observed after 4000 h. At 1000 h, an increase was observed in the height of the carbonyl absorption peak at 1727 cm^{-1}. This increase in carbonyl content at the surface has been attributed to an oxidative photodegradation mechanism. Other authors have observed similar changes in other organic materials [5]. A broadening of the peak at 1605 cm^{-1}, and a decrease in relative intensity of peaks 1509 cm^{-1} and 828 cm^{-1} was also observed. These peaks are all associated with the aromatic ring structure.

SUMMARY

It has been shown that exposure to UV radiation can significantly affect the bulk tensile properties of a vinyl ester resin matrix. The ultimate tensile properties such as ultimate strain and specific toughness were the most sensitive to degradation, with up to a 40% decrease in the ultimate strain and a 60% decrease in specific toughness after 4000 h of exposure in an integrating-sphere-based exposure chamber. Fine scratches observed in the unexposed surface, were depleted while pit defects grew in number and size. The hardness and Young's modulus, as measured by an AFM indentation technique both increased after 1000 h of exposure, but no significant difference was observed between the 1000 h and

4000 h specimens. FTIR-ATR analysis showed evidence of an oxidative photodegradation process. It may be concluded that an increase in surface modulus coupled with an increase in the surface flaw size and population greatly reduced the energy required to nucleate and propagate a crack in tension. Thus, while the degradation may be limited to a thin surface layer, bulk mechanical properties may be greatly affected.

ACKNOWLEDGEMENTS

REFERENCES

1. Martin JW, Chin JW, Byrd WE, Embree E, Kraft KM. *Polymer Degradation and Stability,* 63, 297-304 (1999).
2. VanLandingham MR, McKnight SH, Palmese GR, Elings JR, Huang X, Bogetti TA, Eduljee RF, Gillespie Jr. JW, *J Adhesion,* 1997; 64:31-59.
3. Luoma GA, Rowland RD. *J. Appl. Pol. Sci.*, 32, 5777-5790 (1986).
4. VanLandingham MR, Villarrubia JS, Guthrie WF, Meyers GF; "Nanoindentation of Polymers: An Overview," in *Macromolecular Symposia*, 167: Recent Advances in Scanning Probe Microscopy of Polymers, V. V. Tsukruk and N. D. Spencer, eds. (2001) 15-44.
5. Schoolenberg GE, Vink P. *Polymer,* 32, 432-437 (1991).